Polymer Flow Analysis for Mold Optimization

Northwestern University
ME 378

A collaborative effort between:
Cristian Villazhannay
Corey Wang
Lukas Wolf

1. Introduction

Today's modern world has an abundance of plastic parts, converting injection molding into an ubiquitous part of manufacturing processes all over the world. Injection molding is defined as the process of "shaping rubber and plastic articles by injecting heated material into a cold, closed mold" [11]. To fully comprehend this report, it is essential that the reader hold at least a cursory understanding of the injection molding process. As shown in Fig. 1, a dedicated machine heats plastic granules, turning it into a single polymer melt. A pneumatic or hydraulic screw-ram then acts as a piston, pushing this polymer melt into a part mold through a nozzle. Thus, an injection molded plastic part is born!

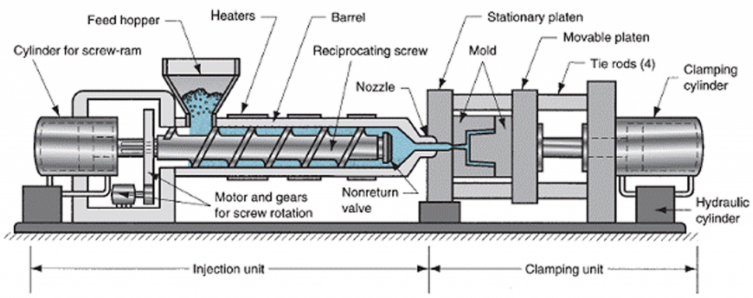

Fig. 1. Injection Molding Machine.
Source: Adapted from [14]

The popularity of injection molding stems largely from the scalability of the operation, and the amazing properties that these engineered plastics hold. Like any manufacturing process, a multitude of variables govern the quality of the output plastic part. These variables include temperature, injection pressure, polymer melting points, injection speed, etc. This report will focus on a critical aspect of the output part: mold design. Fig. ca further elaborates on mold design terminology.

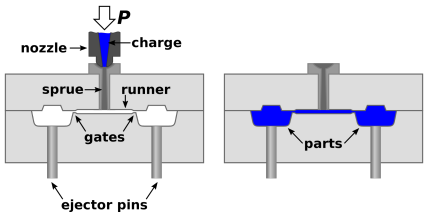

Fig. 2. Mold Terminology Identification.
Source: Adapted from [16]

The runner is a channel that allows plastic material to flow from the sprue to the cavity [9]. The mold cavity is "a shaped cavity used to give a definite form to fluid or plastic material" [8]. This analysis will largely concern itself with modification in the geometrical design of both these items.

This report intends to verify traditional injection molding rules. These rules are not sanctioned by any specific governing body, instead they are simply accepted to be "tried and true" rules. To verify these rules, specific aspects of the mold geometry will be changed — whose effect will

then be measured with quantifiable parameters. These quantifiable parameters usually relate to the velocity, temperature or pressure of the polymer melt.

Additionally, analysis of the importance of the temperature of the polypropylene will be undertaken. We chose to model this by varying the contact angle of our polymer melt with the mold wall (which directly relates to temperature, as shown in figure 4) to observe whether it has any effect on flow and if there are advantages to using a specific material temperature. The variable we will measure will be the flow's average inlet pressure, which should tell us about the pressure difference between the inlet and outlet due to how we define our outlet boundary condition (explained below). One more thing to note is that this experiment has other implications - contact angle also varies depending on how hydrophilic/hydrophobic the mold wall material is, but in our experiment we assume the mold material to be a constant.

Lastly, to perform verification on the results, a Richardson Extrapolation will measure the effect that mesh refinement has on the results. An informal scoping study was also performed to explore the effects of changes in timestep size.

2. Methods

2.1 Problem Statement

As aforementioned, an analysis of traditional injection molding rules is being conducted. However, these rules are often broad and vary from source to source. The rules that will be used as a basis for this analysis will be sourced from a course packet designed by Northwestern University professors [9]. The mold design rules that will be analyzed are:

1. It is best practice to maintain uniform wall thickness.
2. Avoid sharp corners.
3. ~~Usage of a runner well can improve flow performance.~~

Each rule will be verified using a quantitative variable that is significant to flow behavior, which will be elaborated upon in the *Results* section of this report.

2.2 Fluent Models

To model injection molding into a closed mold in ANSYS Fluent, fluid behavior needed to be considered to choose an appropriate model. Since injection molding is a filling operation into an air-filled cavity, a necessity arose for a multiphase model. Ultimately, the Volume of Fluid Multiphase Model (VoF Model) was deemed the most appropriate for the task.

The VoF model is capable of accurately modeling two or more immiscible fluids through the tracking of the volume fraction and momentum equations throughout the domain [6]. In this model, the Navier-Stokes equations (mass, momentum, but no energy equation) are being solved. The volume fraction equation solves for the volume fraction, which represents what percentage of the cell, or mesh element, is filled with a certain fluid. This enables the VoF model to work via

tracking the interface between two distinct fluid elements. It also reinforces the idea why these two fluids must be immiscible for this model to work.

Finally, the last model being used is a Viscosity Model for laminar flow. To determine if injection molding was turbulent or laminar, the team approximated the Reynolds number of this flow using (1). The calculated *Re* was 0.1158, which clearly defines a laminar flow. For the full calculation see Appendix A.

$$Re = \frac{\rho u L}{\mu} \quad (1)$$

2.3 Fluent Solvers

The solution solvers that were used to run the simulations we desired are defined.

General Solution:

1. Pressure Based Solver, Transient Formulation on a Planar Field.
2. Gravity is defined as -9.81 m/s^2

Solution Methods:

1. Pressure-Velocity Coupling: SIMPLE
2. Spatial Discretization
    a. Gradient: Least Squares Cell Based
    b. Pressure: PRESTO!
    c. Momentum: QUICK
    d. Volume Fraction: Compressive
3. Transient Formulation: First Order Implicit

The reason why a pressure-based solver was used instead of a density-based solver (despite the compressive nature of the problem) is because of limitations using the VoF model. In fact, the density-based solver is not available for the VoF model. A transient formulation is utilized because the problem in question would be tracking the interface of the fluid with respect to the time passed. By using a transient solver, the percentage of the mold model can be monitored as it occurs. Finally, gravity is defined since it plays a part in how the fluid settles in the mold since a pressure inlet is not being used.

The solution methods were chosen in order to maximize convergence. The ANSYS tutorial recommends a non-iterative time advancement method with PISO, but this solution was inappropriate for our problem. It simply would not converge over the desired period of time, often failing due to floating point errors. Likewise, when PISO alone was used as an iterative time advancement scheme, the flows were unphysical. To define unphysical flow properties, the fluid would simply float despite gravity being active. An iterative time advancement scheme, like SIMPLE, provided consistent results to solve our problems.

The Spatial Discretization Pressure Method was chosen according to the theory behind the available pressure methods in ANSYS. Only PRESTO! and Body Force methods were available due to the VoF model limitations. According to the ANSYS Theory Manual, the PRESTO! method is recommended for highly curved domains [4]. Due to the twisting channel through which the flow was expected to go through, it seemed that PRESTO! was the ideal option. To

further reinforce this decision, body forces like gravity were not particularly dominant in our expected flow since surface forces like viscosity, pressure, and velocity were driving fluid factors. Convergence was a non-issue.

The Spatial Discretization Momentum Method that was chosen is the QUICK scheme. The First and Second Order Upwinding Schemes were not used since "for simulations using the VoF multiphase model, … upwinding schemes are generally unsuitable … because of their overly diffusive nature" [5]. It is for this same reason that Third Order MUSCL was not used, since it blends a Second Order Upwinding Scheme with another equation. The recommended Modified HRIC Scheme was heavily considered but actually unavailable for our use — see Fig. 3. Therefore, the QUICK scheme was chosen because with implementation of structured meshing, "QUICK will typically be more accurate for structured meshes aligned with flow direction" [5].

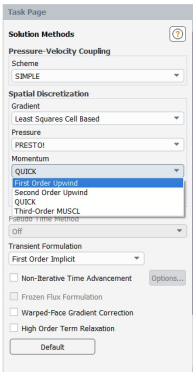

Fig. 3. Available Solution Methods.

The Spatial Discretization Volume Fraction Method used was the Compressive method. This was the result of extensive testing and research. The theoretical basis behind our selection was driven by ANSYS's "Choosing a Volume Fraction Formulation" [3]. The recommended solution for our problem was the CICSAM Method, which was "particularly suited for flow with high viscosity ratios between phases" [3]. However, this solution method had trouble converging once it would pass through the mold gate. Instead, the Compressive method, which is a "reconstruction scheme … based on the slope limiter, … to avoid spurious oscillations" in the solution domain, was employed [2]. This phrase means that the scheme works to maintain the fluid interface as a single body — tamping down droplet formation, air entrapment, and waves [12]. Due to the highly viscous nature of polypropylene, this scheme works well to recreate the expected fluid effects of a highly viscous polymer melt. Not only was interface quality uncompromised, but convergence was no longer an issue as well.

2.4 Materials

The materials used in this analysis are air and polypropylene. For air, the default properties of the "air" material in ANSYS Fluent are used. The polymer chosen was polypropylene (PP), since it is one of the most common injection molding materials [10]. PP has a shear-dependent viscosity, which means the viscosity changes based on the shear stress applied. PP also has strong non-Newtonian flow characteristics, and the viscosity can range from approximately 400 Pa·s to 4000 Pa·s. However, the VoF Model struggles when there is a high viscosity ratio between fluids at the interface. Therefore, the viscosity of the PP was restricted by the limitations of the VOF

Model. In our preliminary experiments, the most realistic flows occurred when a viscosity of 200 Pa·s was used. For PP, a new material was created in Fluent with a viscosity of 200 Pa·s, a surface tension coefficient of 30.8 mN/m, and a density of 905 kg/m^3 [13]. The last property prescribed for PP was the contact angle on the walls. PP has an approximately linear relationship between its temperature and the wall adhesion angle against steel. At our chosen temperature of 250℃, this value is approximately 60° [15].

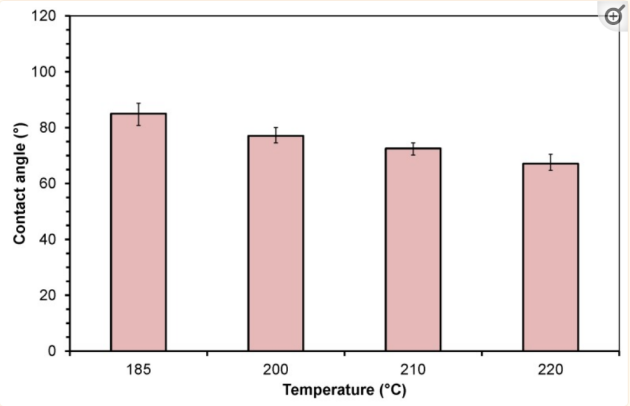

Fig. 4. Contact Angle of Polypropylene on Steel at Different Temperatures.
Source: Adapted from [15]

2.5 Geometries

In order to apply our analysis to future 3D geometries, it was decided that the ANSYS model must be adaptable to imported geometries. Therefore, all geometries were generated in NX, a CAD program, and subsequently imported in ANSYS Workbench. There are numerous advantages to this method, as geometries that are generated in CAD programs are typically easier to modify than those designed in DesignModeller. Please note, however, that all 2D geometries used in the analysis *are* capable of being created in DesignModeller.

For the interested reader, in order to successfully import 2D geometry into ANSYS Workbench, a sketch must first be made in NX and extruded. For continued ease of use, it is recommended to sketch on the XY plane, as the geometry will be automatically oriented to this plane in the Meshing and Solution cells of Fluent. The thickness of this extrude is of no importance. To circumvent licensing issues that prevent the import of native NX .prt files, the extruded geometry must be exported as .igs/.iges file. Once imported, the part can be opened in DesignModeller, where the *Thin* operation can then flatten this 3D geometry into a 2D surface again. Now, the geometry is ready for use!

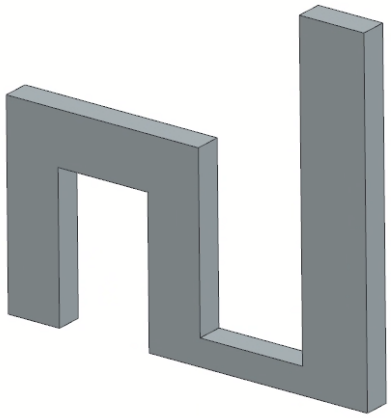

Fig. 5. Extruded NX Geometry Import Conversion.

Injection molding parts can be manufactured up to 4'x4', however each of our geometries were significantly smaller, to model more commonly manufactured parts [1]. In order to base our simulations in reality and prepare for verification, the 2D geometries are adapted cross-sections that utilize the measurements of real molds. An example of an actual cross-section is provided in Fig. cb. All 2D geometries are meant to mimic the flow of polymer melt through this mold cavity cross-section.

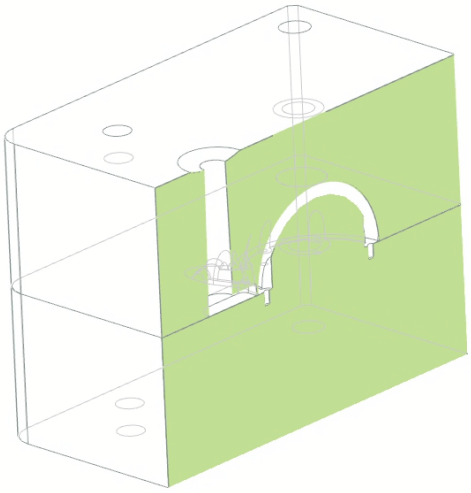

Fig. 5.5. Real Mold Cross-Section.

All geometries are pictured in Figs. 6-8. Dimensions have been purposefully included to aid in recreating the model.

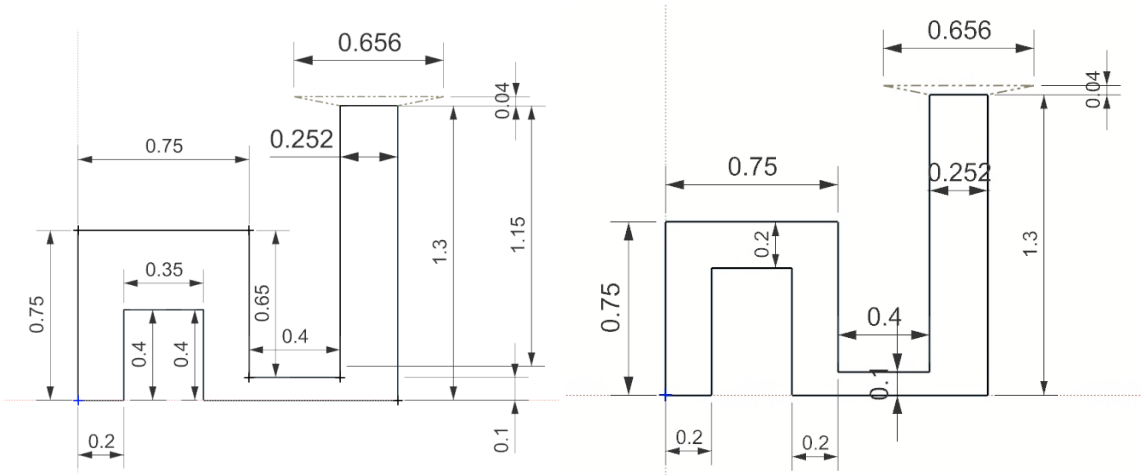

Fig. 6. Non-Uniform Wall Thickness (left), Uniform Wall Thickness (right).

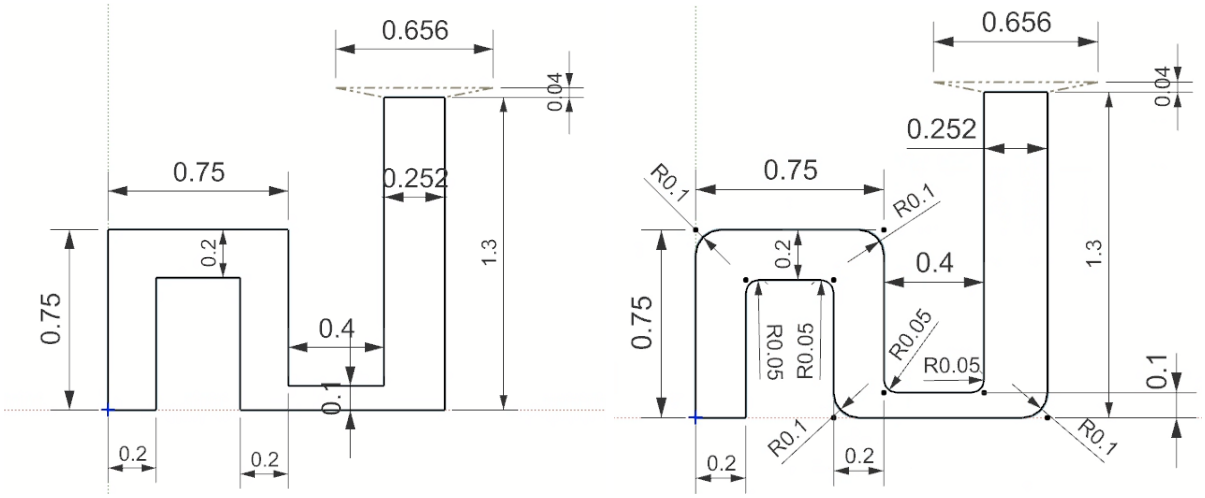

Fig. 7. Sharp Corners (left), Rounded Corners (right).

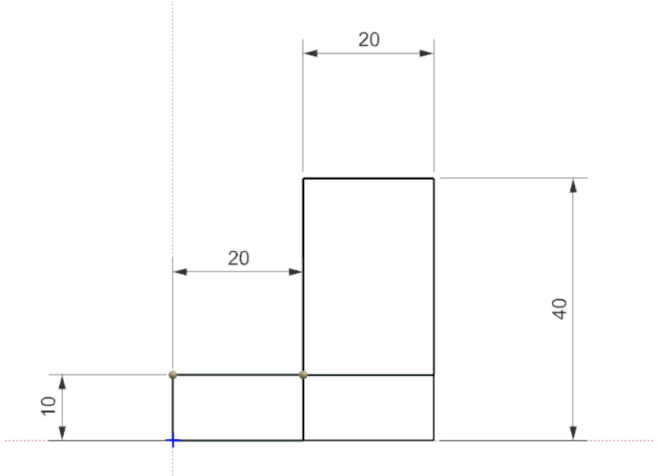

Fig. 8. Contact angle experiment (dimensions in mm).

2.6 Meshes

As previously mentioned, the VoF model works by tracking the interface between two immiscible fluids. At this interface, the model approximates the interface shape by applying a chosen method of interpolation (Geo-Reconstruct, CICSAM, Donor-Acceptor, etc.) to the volume that exists within the interface mesh elements [7]. Since these interpolation models are not infallible, in order to better approximate the interface shape, all meshes used were composed of fine elements. In all meshes, a fine element is one that is 0.0001 m. By using fine elements throughout the entirety of the fluid domain, the interface could be accurately tracked as it moves. The fine element size also helps reduce "smearing" at the interface, which represents solution uncertainty between the position of the two phases.

Due to the rectangular nature of our domain, the team decided to use mapped meshing with quadrilateral elements when possible to simplify post-processing. The usage of a fine mapped mesh was also beneficial to our solution accuracy (see *Fluent Methods*). This decision was largely born out of research oriented to improving solution accuracy. This does not imply that free-meshing or other meshing techniques yielded different results. Further testing may be required to test other free-form meshes.

Our relatively simple geometries meant that mesh refinement for a Richardson extrapolation was feasible. To perform this calculation, a mesh sizing control was implemented into the mesh to allow for easy manipulation of the mesh elements. The geometry used was the rectangular non-uniform wall thickness. Usage of mapped meshing in this case also aided in the uniform scalability of the mesh size. The meshes were scaled with a 1:4 ratio between iterations. The number of elements and nodes are tabulated in Table 1, with the meshes visible in Fig. 9.

Mesh	**Element Size**	**Elements**	**Nodes**
Coarse	0.00050	2564	2396
Medium	0.00025	9964	9625
Fine	0.000125	39539	38868

Table 1: Mesh Sizes

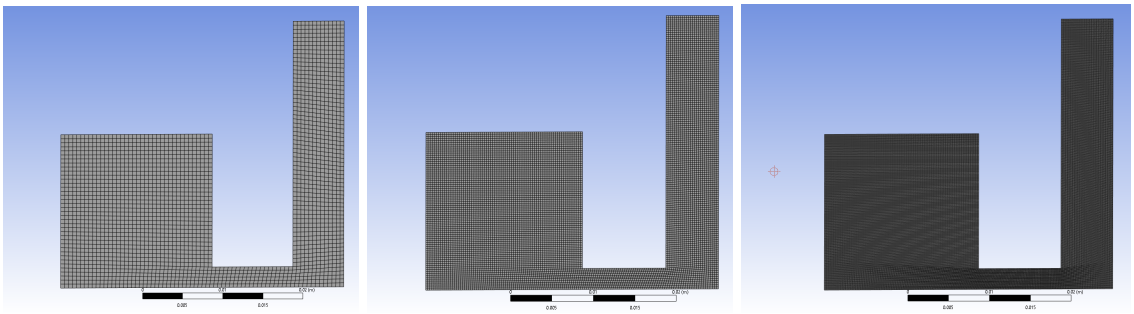

Fig. 9:Course (left), Medium, and Fine (right).

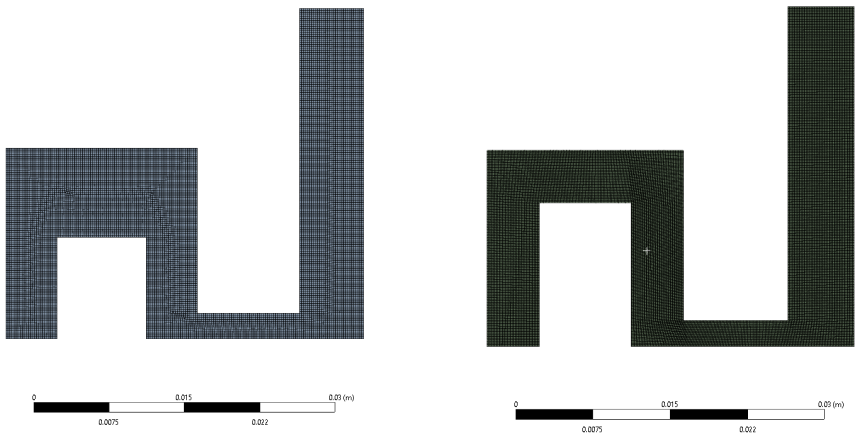

Fig. 10. Non-Uniform Wall Thickness (left), Uniform Wall Thickness (right).

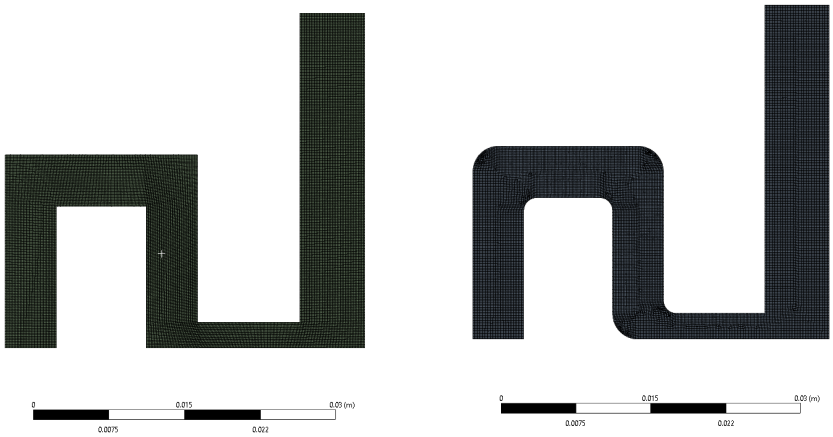

Fig. 11. Sharp Corners (left), Rounded Corners (right).

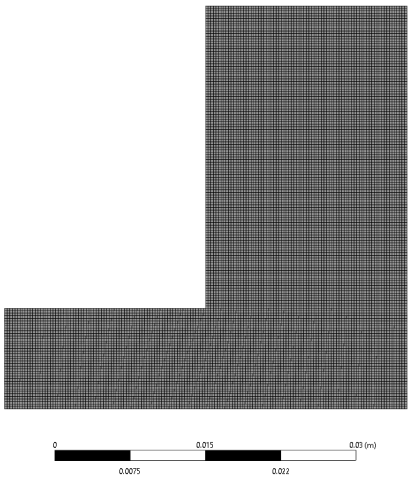

Fig. 12. Contact angle experiment

2.7 Typical Simulation Setup/Boundary Conditions

The timestep decided upon was $5 \cdot 10^{-4}$ seconds for 300 iterations. The overall entire domain is spread over 0.15 seconds. The problem setups are demonstrated in Figs. 13-15. The green grid represents the fluid domain over which this problem is being solved. The highlighted blue line with arrows represents the inlet. The highlighted red line with arrows represents the outlet.

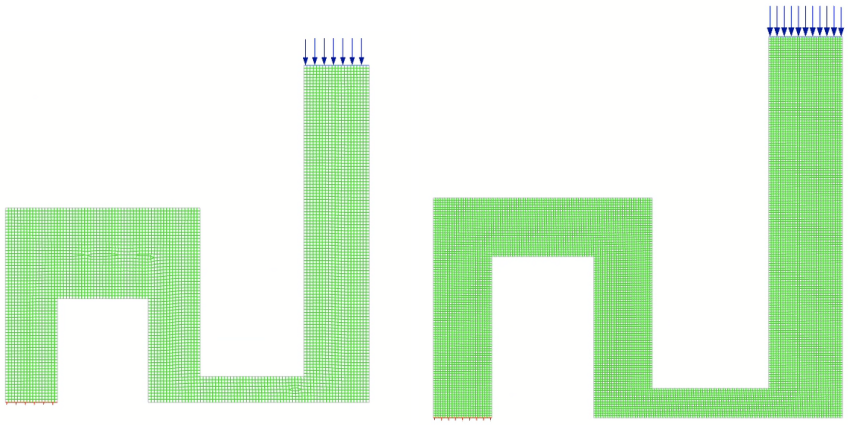

Fig. 13. Non-Uniform Wall Thickness (left), Uniform Wall Thickness (right).

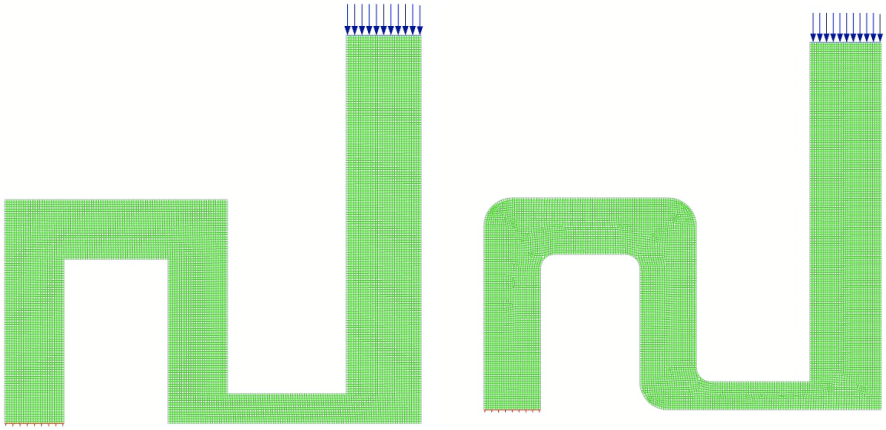

Fig. 14. Sharp Corners (left), Rounded Corners (right).

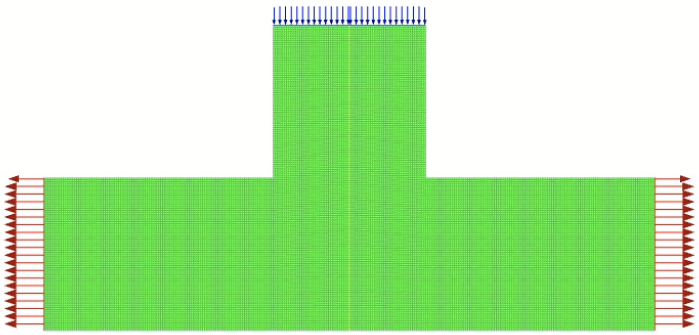

Fig. 15. Contact angle experiment.

The inlet was defined as a velocity inlet at 4 m/s, and the outlet was defined as a pressure outlet at 0 Pa, gage pressure. A velocity inlet was chosen to model the typical injection molding speed of an injection molding machine. A pressure inlet was considered the ideal case, since injection speed is dependent on the injection pressure. However, implementation of a pressure inlet was troublesome, often causing a myriad of issues when attempted.

3. Results

The quantities of interest are fluid velocity and the surface area integral of each fluid phase. The velocity is a measure of the flow's uniform filling throughout the part, and the surface area integral is a measure of the mold's conduciveness to fluid flow. These variables were measured in post-processing in two distinct places, as shown in Fig. 16. We chose these points because of their proximity to contours in the walls, and the changing geometries surrounding them.

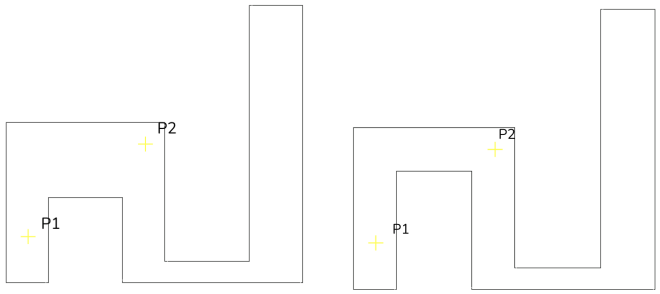

Fig. 16. Measurable Point Geometry.

	X	Y	Z
Point 1 (P1)	0.00242071	0.00428713	0.000160657
Point 2 (P2)	0.0168411	0.0164059	0.000164616

Table 2: Point Coordinates

3.1 Part Thickness Analysis

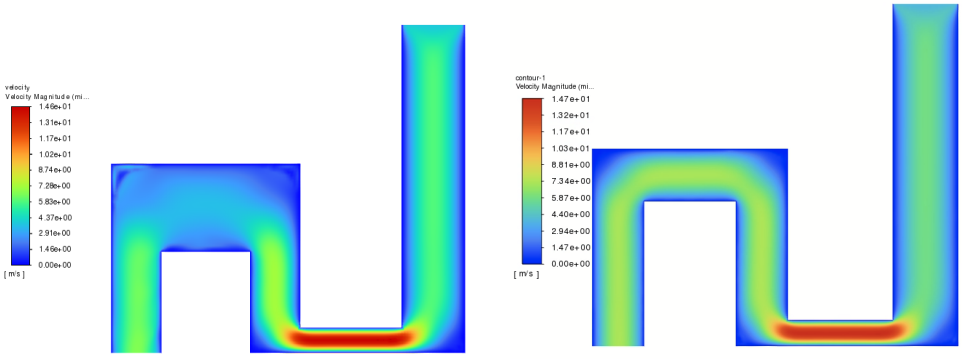

Fig. 17: Velocity Contours.
Non-Uniform Wall Thickness (left), Uniform Wall Thickness (right).

	Non-Uniform	Uniform
Area of Air	8.4%	4.14%
Area of Polypropylene	91.6%	95.85%
Velocity, *m/s* (P1)	6.44234	7.3246
Velocity, *m/s* (P2)	1.7197	3.87759

Table 3: Part Thickness Quantities

The results of these simulations align with our expectation in reality. The non-uniform part thickness does not fill the mold as much as the uniform part. This is shown by the higher percentage of air still present in the mold after the alloted simulation time. Likewise, the velocity of the non-uniform part thickness was greatly affected in areas that were thicker and propagated after, as shown in table 3.

Therefore, the "uniform part wall thickness" rule can be confirmed as the changing velocity in the non-uniform wall thickness means that parts of the mold will cool faster than others due to being filled quicker, which can cause defects and other problems.

3.2 Corner Analysis

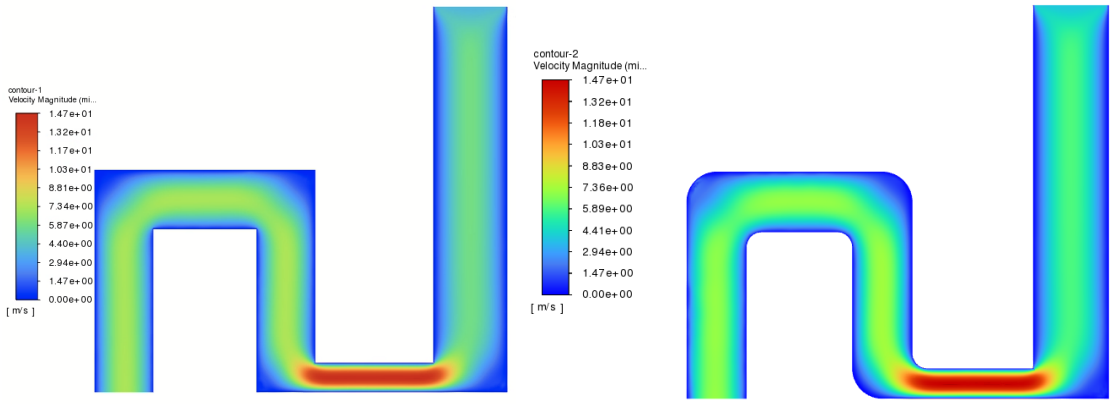

Fig. 18. Velocity Contours.
Sharp Corners (left), Round Corners (right).

	Sharp	Round
Area of Air	4.14%	4.29%
Area of Polypropylene	95.85%	95.71%

Velocity, *m/s* (P1)	7.3246	7.09126
Velocity, *m/s* (P2)	3.87759	3.44144

Table 4: Corner Analysis Quantities

The results of these simulations were surprising, as they contradicted our expectations for these simulations. The rounded corners mold appears to perform worse than the sharp corners mold, shown by the higher percentage of air still present in the mold after the alloted simulation time. This is a very surprising result, because we expected that even if everything else were to be the same, the same amount of polypropylene would take up a larger proportion of the area in the rounded corners geometry simply due to the slightly smaller total area. Likewise, the velocity in the round corners mold was slower than in the sharp corners mold - although not significantly.

Therefore, our experiments disagree with the “avoid sharp corners” rule. The round corners made no significant impact on mold performance. In fact, the round mold was worse than the sharp mold, albeit marginally when it comes to mold-filling. The defining factor in this scenario was the velocity which was about 0.5 m/s faster in the sharp mold! This is an indicator of increased efficiency, which can translate to better cooling.

3.3 Contact Angle Analysis

In our analysis of the contact angle, as described in the methods section, we measured the average inlet pressure at a given time (0.5s, corresponding to 100 timesteps of 0.0005s each) while varying the contact angle.

Contact Angle (°)	Average Inlet Pressure (Pa)
30	2034289
40	2033845
50	2033369
60	2034673
70	2034195
80	2033718
90	2033845
100	2033485
110	2034027
120	2033628
130	2033504
140	2033495
150	2034075

Table 5: Tabulated Values of Avg. Inlet Pressure vs. Contact Angle

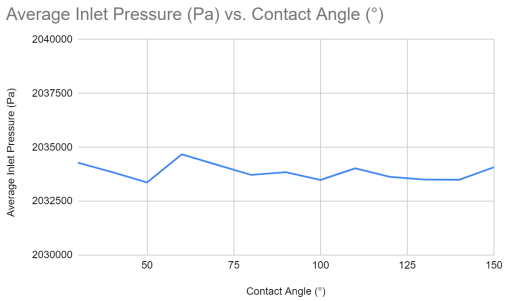

Fig. 18 Plot of Avg. Inlet Pressure vs. Contact Angle

As shown by both the table and plot above, we failed to observe any noticeable trend between our quantity of interest and contact angle. This is a bit surprising, but we suspect that it may be due to our experimental/modeling methodology rather than being a realistic result. Having tried it with velocity, the same trend was observed.

4. Discussion

*4.1 Verification (*Richardson extrapolation)

To perform a Richardson Extrapolation, we chose to use the three meshes noted in Table 1. Using these meshes, we ran the simulation at an inlet velocity of 4 m/s for 10 time steps, each 0.0005 seconds in length. The quantifiable value used for this extrapolation was velocity at (0.015, 0.0025), which is approximately the outlet of the small chute at the bottom of the geometry, just past the peak velocity. This location is shown in Figure 19.

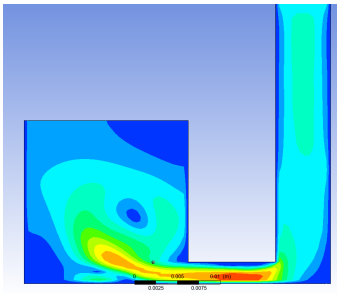

Fig. 19: Location of the velocities taken for Richardson Extrapolation

The values for each mesh are shown in Table 6.

Mesh Size	Flow Velocity (m/s)
Fine	7.97
Medium	7.58
Course	6.75

Table 6: Recorded velocities at (0.015, 0.0025) for each mesh sizing

To continue the extrapolation, we first calculated p - the order of magnitude for the regression. q(p) is 0 in this case, because the refinement factor for each mesh is the same (2). This calculation can be found in (B.1), and the value is found to be 1.08. With this value, we found the extrapolated flow velocity value at this point as 8.25 m/s. This calculation can be seen in (B.2).

To further explore our results, we found the extrapolated relative error in calculation (B.3), which was found to be 3.43%. Further, in calculation (B.4) we explored the grid convergence index, which was found to be 5.42%. All of these values can be found below in Table 7.

N1,N2,N3	2396, 9625, 38,868
r_{21}	2
r_{23}	2
Velocity, Fine Mesh (m/s)	7.969
Velocity, Medium Mesh (m/s)	7.579
Velocity, Coarse Mesh (m/s)	6.749
p	1.08
u_{extra}^{21} (m/s)	8.252
e_{ext}^{21} (%)	3.43
GCI_{fine}^{21} (%)	5.42

Table 7: Results of Richardson Extrapolation

These are all reasonable results, and show a clear trend towards convergence with a decrease in mesh cell dimensions.

4.2 Time Step Analysis

With a transient model the, the time step size on our solution may have significant impacts on the results. To test this, the velocity at the point (0.015, 0.0025 - the same point seen in Figure 19) at several different times, for several different time step sizes (.00025, .0005, .001). Each of these results was taken from a model with 4 m/s inlet velocity run on the non uniform wall thickness geometry. These results are displayed in Figure 20.

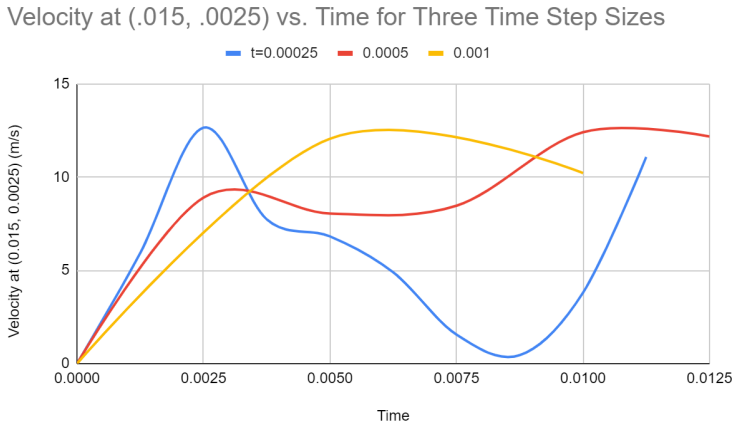

Fig. 20: Velocity trends for different time step sizes

The results of this test show some very interesting results. The trends for time step sizes 0.001s and 0.0005s seem to follow similar trends, while the trend for 0.00025s has a high variance of values. This is the opposite of what we expected, which was that if the time step size was decreased we would see a more obvious trend. However, this also makes sense, as when time step size increases, smearing increases, and the velocities are more likely to directly follow a simple trend instead of having real world variance in velocity values.

4.2 Validation

For basic validation, we looked into the continuity equation, noted in Appendix C. This equation provides a basis for the validation of our model. Comparing the three basic areas of the non uniform wall thickness geometry (.252, .2, and .1 in^2), and the average velocities across the three areas after a significant amount of time has passed (5.06 ,4, and 10.1 m/s). These values line up very well with the expected values found in Appendix C of 5.04, 4, and 10.08 m/s. The slight variations are likely due to mesh and other approximations.

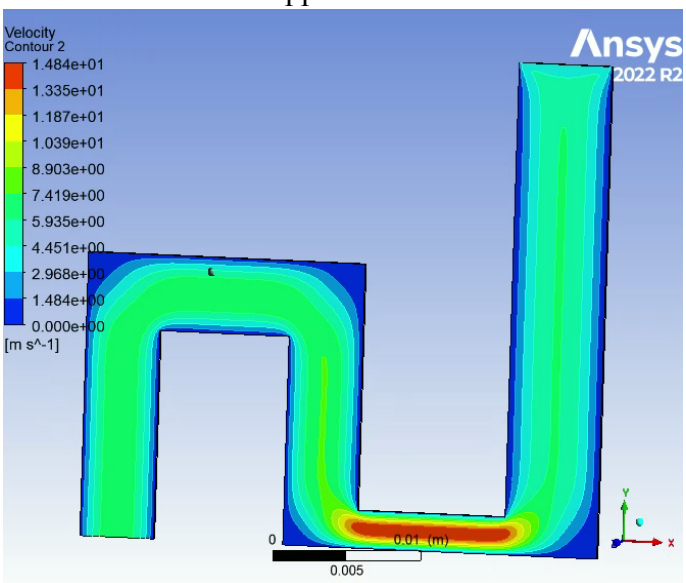

Fig. 21: Velocity Contour of nonuniform thickness walls geometry

In terms of other validation, we primarily observed our results visually to check whether the behavior was realistic. In our animations (presented in our presentation), we observed some encouraging results such as how the viscous fluid moved and stayed as a “blob”, rather than hitting a wall and quickly dispersing which would not be in line with our expectations. Our observations were also in line with how we would expect some defects to form, such as how the fluid front slows down as it moves further into the mold, which is the cause of some defects.

For these reasons, we have reasonable confidence in our simulations despite the approximations made (e.g., using a scaled-down viscosity and consequently, a lower velocity to match) that may not correspond exactly to their real-life values. Despite this, we believe that our modeling of polymer flows is at least somewhat reasonable apart from the contact angle experiment, which we believe requires more work.

For future work, we would like to try creating real-life molds corresponding to the different geometries modeled in our work. We could try experiments with those molds, such as filling them halfway and observing the shapes to see if they correspond to what we saw in our simulations. We would also run the experiments with the non-uniform and uniform wall thicknesses, as well as the sharp/round corners to see how the results differed in each case.

Appendix A

$$Re = \frac{\rho u L}{\mu} \tag{A.1}$$

$$Re = \frac{(905)(4)(0.0064008)}{200} = 0.11584$$

Appendix B

$$p = \frac{1}{ln(r_{21})}\left|\ln\left|\epsilon_{32}/\epsilon_{21}\right| + q(p)\right|$$

$$p = \frac{1}{ln(2)}|\ln|-.83/-.39| + 0| \tag{B.1}$$

$$u_{extra}^{21} = ((r_{21}^{p} \cdot u_1 - u_2)/(r_{21}^{p} - 1)$$

$$u_{extra}^{21} = ((2^{1.08} \cdot 7.969 - 7.579)/(2^{1.08} - 1) \tag{B.2}$$

$$e_{ext}^{21} = \left|\frac{u_{extra}^{21} - u_1}{u_{extra}^{21}}\right|$$

$$e_{ext}^{21} = \left|\frac{8.25 - 7.969}{8.25}\right| \tag{B.3}$$

$$GCI_{fine}^{21} = \frac{1.25}{r_{21}^{p} - 1}\left|\frac{u_1 - u_2}{u_1}\right|$$

$$GCI_{fine}^{21} = \frac{1.25}{2^{1.08} - 1}\left|\frac{7.969 - 7.579}{7.969}\right| \tag{B.4}$$

Appendix C

$$A_1 V_1 = A_2 V_2 \tag{C.1}$$

$2.52*4 = 2*V_2$ (V_2=5.04 m/s)

$2.52*4 = 1*V_3$ (V_3=10.08 m/s)

References

[1] *A guide to sizing injection molding machines | plastics machinery ...* (n.d.). Retrieved March 6, 2023, from https://www.plasticsmachinerymanufacturing.com/injection-molding/article/21151087/a-guide-to-sizing-injection-molding-machines

[2] ANSYS, *ANSYS Fluent Theory Guide v.R12023.* (2023). Accessed Mar. 13, 2023. [Online]. Available: http://www.pmt.usp.br/academic/martoran/notasmodelosgrad/ANSYS%20Fluent%20Theory%20Guide%2015.pdf.

***** The 2013 release is provided here, as the 2023 version is secured behind an account paywall. All conveyed information remains accurate between versions.

[3] ANSYS, "Choosing a Volume Fraction Formulation". Afs.enea.it. https://www.afs.enea.it/project/neptunius/docs/fluent/html/ug/node722.htm. (Accessed Mar. 13, 2023)

[4] ANSYS, "Choosing the Pressure Interpolation Scheme". Afs.enea.it. https://www.afs.enea.it/project/neptunius/docs/fluent/html/ug/node781.htm#pressure-interp-choosing. (Accessed Mar. 13. 2023)

[5] ANSYS, "Spatial Discretization". Afs.enea.it. https://www.afs.enea.it/project/neptunius/docs/fluent/html/th/node366.htm. (Accessed Mar. 13, 2023)

[6] ANSYS, "*Overview and Limitations of the VOF Model*". Afs.enea.it. https://www.afs.enea.it/project/neptunius/docs/fluent/html/th/node298.htm. (accessed Mar. 6. 2023).

[7] ANSYS, "Volume Fraction Equation". Afs.enea.it. https://www.afs.enea.it/project/neptunius/docs/fluent/html/th/node299.htm. (accessed Mar. 6. 2023).

[8] Collins Dictionary, "*Mould".* CollinsDictionary.com. https://www.collinsdictionary.com/us/dictionary/english/mould. (accessed Mar. 6, 2023).

[9] J. Cao, K.F Ehmann, H.Stoll, and M. Beltran. Computer Integrated Manufacturing Course Pack. (2023, Winter). Computer Integrated Manufacturing II. Evanston, IL: Northwestern University.

[10] Midstate Mold and Engineering, "*Most Common Thermoplastics Used in Injection Molding".* Midstatemold.com. https://www.midstatemold.com/common-thermoplastics-injection-molding/. (accessed Mar. 6, 2023).

[11] Oxford English Dictionary*, "Injection Moulding"*. OED.com. *https://www.oed.com/view/Entry/96082?redirectedFrom=injection+molding#eid470132*. (accessed Mar. 5, 2023).

[12] Thomas Frank, "*VOF Compressive Scheme in Fluent*". Researchgate.net. https://www.researchgate.net/post/I_have_a_a_tricky_question_on_the_VOF_compressive_scheme_at_least_with_Fluent. (Accessed Mar. 13, 2023).

[13] Vincent, R., Langlotz, M., & Düngen, M. (2019). Viscosity measurement of polypropylene loaded with blowing agents (propane and carbon dioxide) by a novel inline method. *Journal of Cellular Plastics*, *56*(1), 73–88. https://doi.org/10.1177/0021955x19864400

[14] Xcentric Mold and Engineering, "*Plastic Injection Molding Process"*. Xcentricmold.com. https://www.xcentricmold.com/injection-molding-process/. (accessed Mar. 5, 2023).

[15] Zitzenbacher, G., Dirnberger, H., Längauer, M., & Holzer, C. (2017). Calculation of the contact angle of polymer melts on tool surfaces from viscosity parameters. *Polymers*, *10*(1), 38. https://doi.org/10.3390/polym10010038

[16] *Sprues, Flash, and Runner Explained* (n.d.). Retrieved March 14, 2023, from https://blog.mrt-castings.co.uk/blog/sprues-flash-and-runners-explained